resulting in formation of poly $(A)^+$ histone mRNAs (*18*). We grew 26r and T4V cells in the presence of tet for 40 hours, and, for all four histone genes, ~twofold more poly $(A)^+$ mRNA was recovered from T4V cells than from 26r cells (Fig. 3B, top), and the fraction of histone mRNA in these cells that was poly $(A)^+$ increased 10- to 50-fold (Fig. 3B, bottom).

Histone pre-mRNA 3′ processing requires a complex set of evolutionarily conserved factors, only some of which are shared with the poly $(A)^+$ mRNA 3′ processing machinery (*17*). Using ChIP, we examined recruitment of one common [cleavage polyadenylation specificity factor 100 (CPSF-100)] and one histone-specific [stem loop binding protein (SLBP)] factor to several histone genes and to the *RPLP1* gene. CPSF-100 levels on the *RPLP1* gene peaked at the promoter, consistent with previous observations [e.g., (*19*)], and were equivalent in 26r and T4V cells treated with tet for 30 hours (Fig. 3C, right). On the three histone genes tested, CPSF-100 levels were slightly reduced at the TSS in T4V cells but significantly lower at the 3′ end (Fig. 3C, left), consistent with the defect in 3′ processing. As expected in 26r cells, SLBP was detected at background levels on the *RPLP1* gene (Fig. 3D), whereas significant levels were found associated with the two histone genes tested. However, SLBP levels were significantly reduced both at the TSS and at the 3′ processing site in T4V cells (Fig. 3D). Total levels of SLBP, CPSF-100, and other 3′ processing factors tested were equivalent in the two cell lines (Fig. 2D and fig. S6).

The Thr to Val mutation is a conservative change, and our results thus suggest that modification (e.g., phosphorylation) of Thr^4 is important for its function. To investigate whether Thr^4 is phosphorylated, we used an antibody raised against and specific for a Thr^4-phosphorylated CTD heptad repeat (P-Thr4; fig. S8). Immunoprecipitation (IP)-Westerns with extracts from 26r and T4V cells, using anti-FLAG for IP and P-Thr4 for Western (Fig. 4A), detected a band corresponding to a protein of the expected size in both input and IP from the 26r cells, but this species was detected only at very low levels in the T4V samples, indicating that Thr^4 is phosphorylated in the 26r CTD. Thr^4 is highly conserved throughout eukaryotes, and Western analysis with P-Thr4 of lysates from yeast, fly (KC), 26r, and human (HeLa) cells revealed a band that is the size expected for Thr^4-phosphorylated Rpb1 in all samples (Fig. 4B).

To identify the possible kinase responsible for Thr^4 phosphorylation, we examined whether Thr^4 phosphorylation in DT40 cells was sensitive to the CDK9/P-TEFb inhibitors DRB and flavopiridol (*20*) and found that it was strongly inhibited by both (Fig. 4C and fig. S9). This did not reflect a requirement for prior Ser^2 phosphorylation, because Thr^4 phosphorylation was detected in DT40-Rpb1 cells expressing an Rpb1 derivative with all Ser^2 residues mutated to Ala^2 (S2A) (Fig. 4D). Linking this to the defect in histone mRNA processing in T4V cells, histone mRNA levels in flavopiridol-treated 26r cells were reduced to levels found in T4V cells (fig. S10). Consistent with this, knockdown of CDK9 in human embryonic kidney 293 cells was previously shown to impair SLBP recruitment to histone genes and lead to accumulation of poly $(A)^+$ histone mRNA (*21*).

Our experiments have provided insight into the intricate mechanisms used by cells to couple transcription by RNAP II to subsequent RNA processing. Our data provide evidence that histone mRNA 3′ end formation specifically requires Thr^4 phosphorylation, but it is likely that this modification is important for other CTD functions. Although our experiments have not uncovered evidence for this, the fact that Thr^4 is phosphorylated in yeast, which produces histone mRNA 3′ ends by the same mechanism as other mRNAs, suggests the existence of additional functions in mRNA synthesis and/or processing.

References and Notes

1. Y. Hirose, J. L. Manley, *Genes Dev.* **14**, 1415 (2000).
2. T. Maniatis, R. Reed, *Nature* **416**, 499 (2002).
3. M. J. Moore, N. J. Proudfoot, *Cell* **136**, 688 (2009).
4. P. Komarnitsky, E. J. Cho, S. Buratowski, *Genes Dev.* **14**, 2452 (2000).
5. S. C. Schroeder, B. Schwer, S. Shuman, D. L. Bentley, *Genes Dev.* **14**, 2435 (2000).
6. S. H. Ahn, M. Kim, S. Buratowski, *Mol. Cell* **13**, 67 (2004).
7. Z. Ni, B. E. Schwartz, J. Werner, J.-R. Suarez, J. T. Lis, *Mol. Cell* **13**, 55 (2004).
8. R. D. Chapman *et al.*, *Science* **318**, 1780 (2007).
9. S. Egloff *et al.*, *Science* **318**, 1777 (2007).
10. R. Baskaran, M. E. Dahmus, J. Y. J. Wang, *Proc. Natl. Acad. Sci. U.S.A.* **90**, 11167 (1993).
11. H. Sakurai, A. Ishihama, *Genes Cells* **7**, 273 (2002).
12. J. Wang, Y. Takagaki, J. L. Manley, *Genes Dev.* **10**, 2588 (1996).
13. Y. Takagaki, J. L. Manley, *Mol. Cell* **2**, 761 (1998).
14. J. Wang, S. H. Xiao, J. L. Manley, *Genes Dev.* **12**, 2222 (1998).
15. R. D. Chapman, M. Conrad, D. Eick, *Mol. Cell. Biol.* **25**, 7665 (2005).
16. C. Y. Chen, L. W. Forman, D. V. Faller, *Mol. Cell. Biol.* **16**, 6582 (1996).
17. W. F. Marzluff, E. J. Wagner, R. J. Duronio, *Nat. Rev. Genet.* **9**, 843 (2008).
18. K. D. Sullivan, T. E. Mullen, W. F. Marzluff, E. J. Wagner, *RNA* **15**, 459 (2009).
19. O. Rozenblatt-Rosen *et al.*, *Proc. Natl. Acad. Sci. U.S.A.* **106**, 755 (2009).
20. S. H. Chao, D. H. Price, *J. Biol. Chem.* **276**, 31793 (2001).
21. J. Pirngruber *et al.*, *EMBO Rep.* **10**, 894 (2009).

Acknowledgments: We thank T. Kashima for plasmids and help with construction of the DT40-Rpb1 cell line, W. Marzluff for the SLBP antibody, Z. Dominski for the Lsm11 antibody, and Novus Biologicals for the P-Thr4 antibody. This work was supported by NIH grant R01 GM28983.

Supporting Online Material

www.sciencemag.org/cgi/content/full/334/6056/683/DC1
Materials and Methods
Figs. S1 to S10
References

24 March 2011; accepted 29 August 2011
10.1126/science.1206034

Drosophila CENH3 Is Sufficient for Centromere Formation

María José Mendiburo,[1,2] Jan Padeken,[1,2] Stefanie Fülöp,[3] Aloys Schepers,[3] Patrick Heun[1,4]*

CENH3 is a centromere-specific histone H3 variant essential for kinetochore assembly. Despite its central role in centromere function, there has been no conclusive evidence supporting CENH3 as sufficient to determine centromere identity. To address this question, we artificially targeted *Drosophila* CENH3 (CENP-A/CID) as a CID-GFP-LacI fusion protein to stably integrated lac operator (lacO) arrays. This ectopic CID focus assembles a functional kinetochore and directs incorporation of CID molecules without the LacI-anchor, providing evidence for the self-propagation of the epigenetic mark. CID-GFP-LacI–bound extrachromosomal lacO plasmids can assemble kinetochore proteins and bind microtubules, resulting in their stable transmission for several cell generations even after eliminating CID-GFP-LacI. We conclude that CID is both necessary and sufficient to serve as an epigenetic centromere mark and nucleate heritable centromere function.

The centromere ensures correct segregation of chromosomes during mitosis by providing the site for kinetochore assembly and microtubule attachment. Most eukaryotic organisms contain only one centromere per chromosome, which is specifically positioned and faithfully propagated through each cell cycle. With the exception of *Saccharomyces cerevisiae*, DNA sequence is considered neither necessary nor sufficient to mark centromeres in most eukaryotes, suggesting that centromere identity in many organisms is determined epigenetically (*1*). CENH3 (CENP-A in mammals, CID in *Drosophila*) is a centromere-specific histone H3 variant that replaces canonical histone H3 in centromeric nucleosomes. It is essential for centromere function and kinetochore assembly (*2*–*5*)

[1]Max Planck Institute of Immunobiology, Stübeweg 51, 79108 Freiburg, Germany. [2]Albert-Ludwigs-Universität, Freiburg, Germany. [3]Department of Gene Vectors, Helmholtz Center Munich, German Research Center for Environmental Health, Marchioninistrasse 25, 81377 Munich, Germany. [4]BIOSS Centre for Biological Signalling Studies, Albert-Ludwigs-Universität, Freiburg, Germany.

*To whom correspondence should be addressed. E-mail: heun@ie-freiburg.mpg.de

and thus a prime candidate epigenetic mark for determining centromere identity.

Global misincorporation of CID into chromosome arms leads to the formation of functional ectopic kinetochores only in a small subset of sites (*6*, *7*), hindering a direct correlation between CID presence and kinetochore formation. To determine whether CID is sufficient for directing kinetochore assembly and nucleate centromere identity, we targeted a CID-GFP-Lac Repressor (LacI) fusion protein to an array of lac operator (lacO) sequences stably integrated in *Drosophila* Schneider S2 cells (Fig. 1A and fig. S1B). Inducible CID-GFP-LacI or GFP-LacI fusion proteins are efficiently targeted to lacO sequences only upon pulse induction (Fig. 1B), whereas low leaky expression of CID-GFP-LacI in uninduced cells correlates with an exclusive centromere localization (Fig. 1B and fig. S1A).

CENH3 has been shown to adopt a specialized nucleosomal structure, which is proposed to mark centromeric chromatin (*8*–*14*). To determine whether CID-GFP-LacI is incorporated in nucleosomes at the lacO, mononucleosomes from GFP-LacI and CID-GFP-LacI cells were separated on a sucrose gradient. Analysis of the fractions from both cell lines revealed that lacO DNA comigrates with fractions containing H3-nucleosomes, suggesting that they are chromatinized (fig. S2, A and B). GFP-LacI did not comigrate with nucleosomes, likely due to its release from lacO binding after micrococcal nuclease treatment. In contrast, CID-GFP-LacI was found in nucleosome-containing fractions, indicating that it can interact with chromatin independently of the LacI binding. Nucleosome incorporation was confirmed by coimmunoprecipitation of CID-GFP-LacI with histone H2A in the nucleosome fraction (fig. S2C). To exclude that CID-GFP-LacI migration pattern is only due to the contribution of protein localized to endogenous centromeres, we created a mutant CID fused to GFP-LacI that does not target to centromeres and is therefore present only at the lacO array (fig. S2E). In this mutated protein, three amino acids [G175S, L177V, and L178M (CIDsvm)] in the CENP-A targeting domain (CATD) of CID are replaced by the corresponding residues of histone H3.1, as shown previously for human CENP-A (*15*) (fig. S2D). The migration pattern of CIDsvm-GFP-LacI in sucrose gradients resembles that of CID-GFP-LacI (fig. S2A), supporting the notion that CID-GFP-LacI is in nucleosomes also at lacO regions.

Targeting of CID-GFP-LacI, but not GFP-LacI, to the lacO recruited kinetochore proteins, such as CENP-C and the microtubule-binding protein NDC80/HEC1, 1 day after pulse induction (Fig. 1, C to E) (*13*, *14*, *16*). Probing for the spindle assembly checkpoint proteins POLO kinase and MAD2 revealed the same pattern, suggesting that ectopically targeted CID is sufficient to direct kinetochore assembly (Fig. 1E and fig. S1, C and D).

The formation of a functional ectopic kinetochore at the lacO is expected to generate a dicentric chromosome causing chromosome breakage and anaphase defects (*12*). Indeed, we observe a higher number of aberrant mitotic chromosome configurations in cells expressing CID-GFP-LacI compared with control GFP-lacI cells and containing the lacO array (Fig. 2).

The epigenetic model for centromere identity predicts that a functional centromere self-directs the loading of new centromeric marks after each cell division (*1*). If CID-GFP-LacI identifies the lacO as a centromere, CID molecules without a LacI fusion should also be recruited to lacO

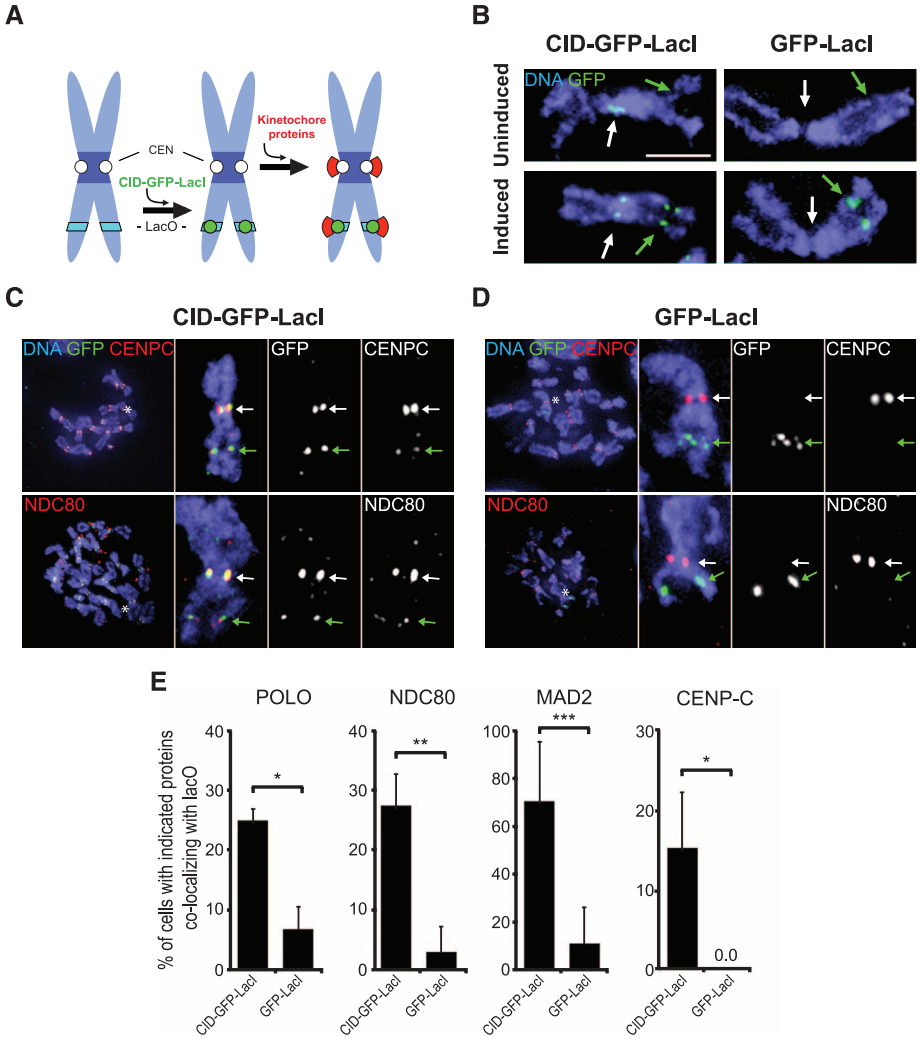

Fig. 1. CID-GFP-LacI is efficiently targeted to lacO sequences and induces kinetochore assembly. (**A**) Schematic representation of the experimental setup. (**B**) Examples of the lacO-containing chromosome 3 from fixed mitotic CID-GFP-LacI and GFP-LacI cells before and after induction with $CuSO_4$ are shown. (**C**) Fixed mitotic chromosomes of CID-GFP-LacI cells were processed 1 day after pulse induction for immunofluorescence (IF) with antibodies to GFP and CENP-C or NDC80. The lacO-containing chromosome is indicated by an asterisk and shown magnified in the right panels. (**D**) Same as on (B), with GFP-LacI cells 1 day after the pulse induction. (**E**) Quantification of the percentage of cells showing colocalization between GFP and different kinetochore proteins in the lacO for the CID-GFP-LacI and GFP-LacI cells similar to (A), (B), and fig. S2, A and B. Values are average ± SD of at least three independent experiments. CENP-C, $n_{\text{CID-GFP-LacI}} = 33$, $n_{\text{GFP-LacI}} = 43$. MAD2, $n_{\text{CID-GFP-LacI}} = 38$, $n_{\text{GFP-LacI}} = 37$. POLO, $n_{\text{CID-GFP-LacI}} = 36$, $n_{\text{GFP-LacI}} = 56$. NDC80, $n_{\text{CID-GFP-LacI}} = 33$, $n_{\text{GFP-LacI}} = 52$. *, $P < 0.05$; **, $P < 0.005$; ***, $P < 0.0005$ (two-sided Fisher's exact test). White arrows indicate endogenous centromeres and green arrows the lacO integration in all panels. Scale bars, 3 μm.

regions. To investigate this, we created a stable cell line containing both an inducible CID-GFP-LacI and a constitutively expressed CID-hemagglutinin (HA) HA construct. Upon pulse induction and targeting of CID-GFP-LacI, we found a low initial CID-HA recruitment to the lacO (9.7%) (Fig. 3A), increasing by two-fold 7 days later (24%) (Fig. 3B). Higher-resolution analysis using stretched chromatin fibers revealed that at initial time points CID-HA localization is restricted to the lacO region (fig. S3A), whereas 7 days after pulse induction, CID-HA (Fig. 3C) or CID (fig. S3B) is also found spreading into adjacent regions (Fig. 3D). CID-HA or CID were never found in lacO sequences in the presence of GFP-LacI (fig. S3C).

CID-GFP-LacI targeting to an ectopic chromosomal locus results in mitotically unstable dicentric chromosomes, hindering the analysis of long-term inheritance of the centromere function. To directly test de novo centromere heritability, we analyzed whether CID-GFP-LacI targeting confers mitotic stability to a centromere-devoid episomal DNA element carrying lacO sequences and a G418-resistance cassette. This plasmid was transfected into S2 cell lines constitutively expressing low levels of either CID-GFP-LacI or GFP-LacI and kept under selection pressure for 28 days (Fig. 4A) (*17*, *18*). The initial transfection efficiency was comparable in both cell lines (Fig. 4B, *–DpnI*). However, we observed a decline in the amount of replicated plasmids (*+DpnI*) in GFP-LacI–expressing cells, whereas CID-GFP-

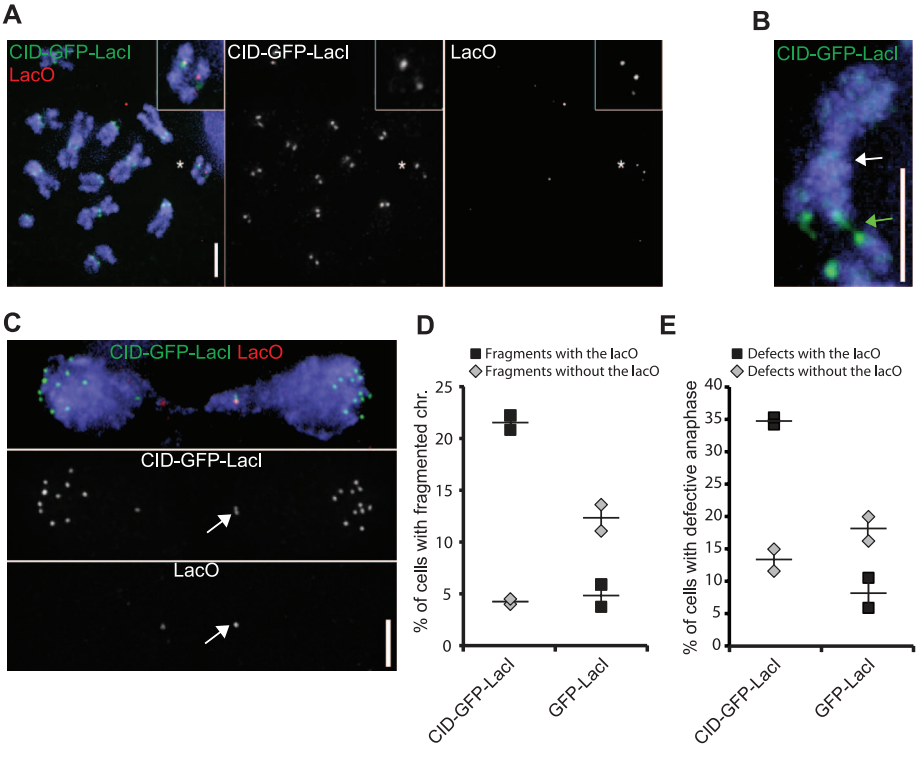

Fig. 2. The lacO-containing chromosome is involved in mitotic defects and fragmentation. (**A**) IF fluorescence in situ hybridization (IF-FISH) on fixed mitotic chromosomes of CID-GFP-LacI cells 1 day after induction reveals a GFP-positive lacO-containing fragment (indicated by an asterisk and magnified in the insets). (**B**) Example of a mitotic chromosome breaking within the lacO sequence upon CID-GFP-LacI targeting (green arrow). The white arrow indicates the endogenous centromere. (**C**) Lagging chromosome containing CID-GFP-LacI colocalizing with lacO sequences (white arrow). Grayscale images of individual channels are shown below. Scale bars, 3 μm. (**D**) Frequency of anaphase figures with defects involving lacO sequences as shown in (C). Horizontal bars are average of two independent experiments. $n_{\text{CID-GFP-LacI}} = 48$, $n_{\text{GFP-LacI}} = 109$. (**E**) Fragmented lacO-containing chromosomes in CID-GFP-LacI and GFP-LacI cells as shown in (A) and (B). Values are average ± SD of at least two independent experiments. $n_{\text{CID-GFP-LacI}} = 42$, $n_{\text{GFP-LacI}} = 47$. *, $P < 0.05$; **, $P < 0.005$ (two-sided Fisher's exact test).

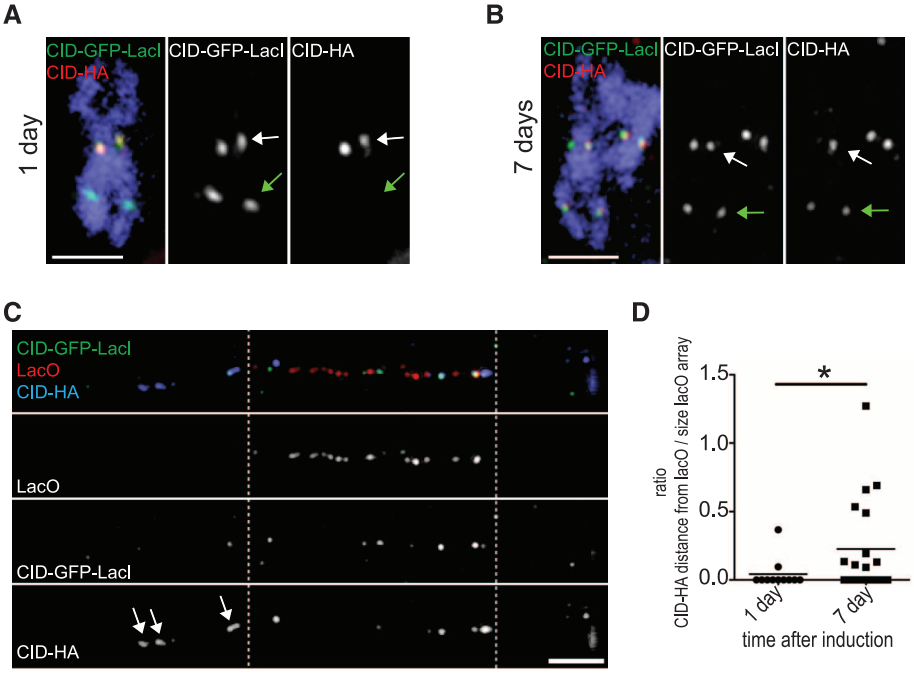

Fig. 3. CID tethered to lacO sites creates a self-propagating epigenetic mark. CID-GFP-LacI expression was induced in the presence of constitutively low levels of CID-HA. Representative images of mitotic chromosomes 1 day (**A**) and 1 week (**B**) after pulse induction are shown. White arrows indicate endogenous centromeres, green arrows the lacO site. The percentages of cells where CID-GFP-LacI sites colocalize with CID-HA are shown. $n_{1\text{day}} = 143$, $n_{7\text{days}} = 29$. (**C**) IF-FISH on a stretched chromatin fiber 1 week after pulse induction. White arrows indicate spreading CID-HA. Dashed white lines delimit the lacO sequence. Scale bars, 3 μm. (**D**) The distance between the most distal HA signal relative to the lacO was measured and normalized to the size of the lacO FISH signal to correct for differential stretching. $n_{1\text{day}} = 11$, $n_{7\text{days}} = 19$. *, $P < 0.05$ (two-tailed Student's *t* test).

LacI cells maintained the plasmid until the end of the experiment (Fig. 4B, +*DpnI*). Efficient replication and proper segregation are the two major factors defining the stability of plasmids (*18*). For the first 7 days, both cell lines replicated the plasmid with similar efficiency (Fig. 4B and fig. S5, F and G), indicating that correct segregation is the main factor contributing to its maintenance in CID-GFP-LacI cells. This was also observed when selection was removed after 16 days or never applied (fig. S5E). Furthermore, we find CENP-C, NDC80, and microtubule connections localizing to CID-GFP-LacI–bound lacO plasmids in mitosis (Fig. 4, C and D, and fig. S4, A and C). These plasmids separate earlier than endogenous chromosomes and generally display a symmetric distribution on the spindle poles (fig. S4, B and C). GFP-LacI cells grew poorly after transfection, and the few mitotic cells detected showed no colocalization of GFP-positive lacO plasmids with either CENP-C or NDC80 (fig. S4D). Further characterization of recovered plasmids showed that plasmid size remained stable except for variability in the repetitive lacO array and did not acquire endogenous *Drosophila* sequences (fig. S5, A to C). A minor fraction of concatenated plasmids did not correlate with efficient recruitment of kinetochore proteins (fig. S5D).

The centromeric mark can self-propagate in the lacO plasmid, as shown by the recruitment of CID-HA to targeted CID-GFP-LacI plasmids and the spreading of both into backbone sequences (Fig. 4E and figs. S5C and S6A). To determine whether centromeric chromatin is inherited even after removal of CID-GFP-LacI targeting, we transiently cotransfected the lacO plasmid and a CID-GFP-LacI expression construct to deliver an initial expression pulse that is progressively lost. Episomal lacO plasmids were detected as nonchromosomal CID/CENP-C foci, with or without a GFP signal. Early after transfection, we found cells that contained both GFP-positive and -negative foci (green bars in Fig. 4F) and a smaller cell population that had already lost CID-GFP-LacI expression but contained nonchromosomal CID/CENP-C foci (black bars in Fig. 4F). The percentage of these GFP-negative plasmids increased until day 27, when all detected CID/CENP-C foci were devoid of any GFP signal (Fig. 4F and fig. S6, B to E). We conclude that an initial targeting of CID-GFP-LacI to the lacO plasmid enables the nucleation of centromere function, which is maintained independently of CID-GFP-LacI expression and targeting.

In recent years, functional biosynthetic kinetochores have been constructed by targeting kinetochore components (*19*–*21*) and chromatin modifiers (*22*, *23*) to minichromosomes. Even though the possibility of bypassing CENH3 chromatin for the assembly of a kinetochore suggested that CENH3 is dispensable for this function (*21*), no evidence of centromere heritability was provided by these studies. Recent reports showing CENP-A–dependent kinetochore formation in vitro (*24*) or by artificially targeting the CENP-A loading factor in humans (HJURP) (*25*) further stress the importance of CENH3 in kinetochore assembly. The results presented here show that CENH3 behaves as a true centromeric epigenetic mark not only by being sufficient for the recruitment of kinetochore proteins during mitosis but also for directing its own incorporation and maintaining centromere function through each cell division.

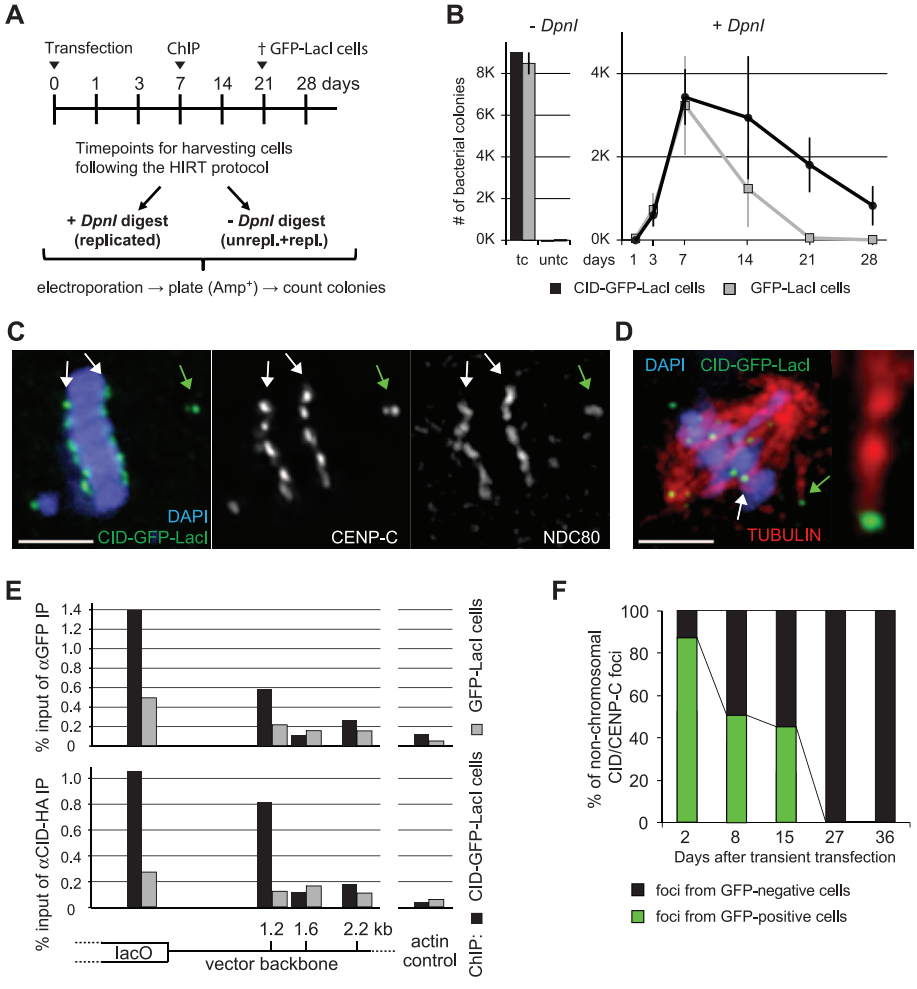

Fig. 4. CID-GFP-LacI confers stability to episomal lacO plasmids and allows epigenetic inheritance of centric chromatin after its elimination. (**A**) Schematic representation of the plasmid rescue assay. (**B**) The average of three independent plasmid rescue experiments is shown ± SEM. tc, transfection control; utc, untransfected control. K = ×1000. (**C**) Immunostainings of CID-GFP-LacI cells in metaphase 9 days after transfection with a lacO plasmid. (**D**) Similar to (C), showing microtubule-plasmid attachments. (**E**) Cells described in (A) were cotransfected with a CID-HA expression construct and the lacO plasmid and subjected to αHA and αGFP–chromatin immunoprecipitation experiments 6 days later. (**F**) Quantification of the percentage of extrachromosomal CID/CENP-C foci in mitotic cells after transient cotransfection of lacO and CID-GFP-LacI constructs. Black: GFP-negative CID/CENP-C foci coming from GFP-negative cells. Green: Foci from cells that contain at least one GFP-positive focus (GFP-positive cells). Scale bars, 3 μm.

References and Notes

1. R. C. Allshire, G. H. Karpen, *Nat. Rev. Genet.* **9**, 923 (2008).
2. M. R. Przewloka *et al.*, *PLoS ONE* **2**, e478 (2007).
3. V. Régnier *et al.*, *Mol. Cell. Biol.* **25**, 3967 (2005).
4. M. D. Blower, G. H. Karpen, *Nat. Cell Biol.* **3**, 730 (2001).
5. L. E. Jansen, B. E. Black, D. R. Foltz, D. W. Cleveland, *J. Cell Biol.* **176**, 795 (2007).
6. P. Heun *et al.*, *Dev. Cell* **10**, 303 (2006).
7. A. M. Olszak *et al.*, *Nat. Cell Biol.* **13**, 799 (2011).
8. T. Furuyama, S. Henikoff, *Cell* **138**, 104 (2009).
9. Y. Dalal, H. Wang, S. Lindsay, S. Henikoff, *PLoS Biol.* **5**, e218 (2007).
10. N. Sekulic, E. A. Bassett, D. J. Rogers, B. E. Black, *Nature* **467**, 347 (2010).
11. B. E. Black *et al.*, *Nature* **430**, 578 (2004).
12. B. McClintock, *Genetics* **26**, 234 (1941).
13. I. M. Cheeseman, A. Desai, *Nat. Rev. Mol. Cell Biol.* **9**, 33 (2008).
14. D. R. Foltz *et al.*, *Nat. Cell Biol.* **8**, 458 (2006).
15. B. E. Black *et al.*, *Mol. Cell* **25**, 309 (2007).
16. R. D. Vierstra, J. Callis, *Plant Mol. Biol.* **41**, 435 (1999).
17. B. Hirt, *J. Mol. Biol.* **26**, 365 (1967).
18. D. Pich, S. Humme, M. P. Spindler, A. Schepers, W. Hammerschmidt, *Nucleic Acids Res.* **36**, e83 (2008).
19. S. Lacefield, D. T. Lau, A. W. Murray, *Nat. Cell Biol.* **11**, 1116 (2009).
20. E. Kiermaier, S. Woehrer, Y. Peng, K. Mechtler, S. Westermann, *Nat. Cell Biol.* **11**, 1109 (2009).
21. K. E. Gascoigne *et al.*, *Cell* **145**, 410 (2011).
22. M. Nakano *et al.*, *Dev. Cell* **14**, 507 (2008).
23. A. Kagansky *et al.*, *Science* **324**, 1716 (2009).
24. A. Guse, C. W. Carroll, B. Moree, C. J. Fuller, A. F. Straight, *Nature* **477**, 354 (2011).
25. M. C. Barnhart *et al.*, *J. Cell Biol.* **194**, 229 (2011).

Acknowledgments: We thank G. H. Karpen, A. Straight, T. Maresca, E. Salmon, C. Sunkel, S. Heidmann, and C. Lehner for reagents. We also thank L. Jansen for critical reading of the manuscript and the members of the Grosschedl Department, particularly S. Chlamydas for pioneering experiments and A. Olszak, H.-J. Schwarz, D. Venegas, S. Daujat, S. Saccani, and D. van Essen for reagents and helpful discussions. A.S. is supported by the Sonderforschungsbereich (SFB) 646, SFB/TR05, and Schwerpunktprogramm 1230 of the Deutsche Forschungsgemeinschaft. P.H. is funded by the Max Planck Society, the Human Frontier Science Program (Career Development Award; CDA), and the Excellence Initiative of the German Federal and State Governments (EXC 294). M.-J.M. and J.P. are grateful for an International Max Planck Research School (IMPRS) fellowship provided by the Max Planck Institute of Immunobiology and Epigenetics.

Supporting Online Material
www.sciencemag.org/cgi/content/full/334/6056/686/DC1
Materials and Methods
Figs. S1 to S6
References (*26*, *27*)

12 April 2011; accepted 19 September 2011
10.1126/science.1206880

Exercise and Genetic Rescue of SCA1 via the Transcriptional Repressor Capicua

John D. Fryer,[1]* Peng Yu,[1] Hyojin Kang,[1] Caleigh Mandel-Brehm,[1] Angela N. Carter,[2] Juan Crespo-Barreto,[1]† Yan Gao,[1] Adriano Flora,[1] Chad Shaw,[1,3] Harry T. Orr,[4] Huda Y. Zoghbi[1,2,5,6,7]‡

Spinocerebellar ataxia type 1 (SCA1) is a fatal neurodegenerative disease caused by expansion of a translated CAG repeat in Ataxin-1 (ATXN1). To determine the long-term effects of exercise, we implemented a mild exercise regimen in a mouse model of SCA1 and found a considerable improvement in survival accompanied by up-regulation of epidermal growth factor and consequential down-regulation of Capicua, which is an ATXN1 interactor. Offspring of Capicua mutant mice bred to SCA1 mice showed significant improvement of all disease phenotypes. Although polyglutamine-expanded Atxn1 caused some loss of Capicua function, further reduction of Capicua levels—either genetically or by exercise—mitigated the disease phenotypes by dampening the toxic gain of function. Thus, exercise might have long-term beneficial effects in other ataxias and neurodegenerative diseases.

Spinocerebellar ataxia type 1 (SCA1) is characterized by a progressive loss of motor skills, usually beginning with impaired gait and balance (*1*). As with other neurodegenerative diseases, the disease protein Ataxin-1 (ATXN1) is abundantly expressed in most neurons, yet some neuronal populations are more vulnerable than others. In SCA1, cerebellar Purkinje cells are first to show dysfunction; eventually, other neuronal populations—including deep cerebellar and brainstem nuclei—are affected, leading to premature death (*2*). Although exercise has beneficial effects on many brain functions (*3*), it is not clear whether it would be protective in SCA1 or would accelerate neuronal demise by increasing the activity and metabolic demands on these already vulnerable neuronal populations, as has been suggested for other neurodegenerative diseases (*4*, *5*).

To determine the effects of exercise in SCA1, we implemented a mild exercise regimen in Atxn1^{154Q} knock-in mice, which bear 154 CAG repeats targeted into the endogenous mouse locus so as to create a model that recapitulates all aspects of SCA1 (*6*). From 4 to 8 weeks of age, wild-type (WT) or Atxn1^{154Q} mice were placed on a fixed-speed rotarod apparatus five times per week, whereas control mice were placed on an

[1]Department of Molecular and Human Genetics, Baylor College of Medicine, Houston, TX 77030, USA. [2]Department of Neuroscience, Baylor College of Medicine, Houston, TX 77030, USA. [3]Stem Cells and Regenerative Medicine Center, Baylor College of Medicine, Houston, TX 77030, USA. [4]Institute of Translational Neuroscience, University of Minnesota, Minneapolis, MN 55455, USA. [5]Program in Developmental Biology, Baylor College of Medicine, Houston, TX 77030, USA. [6]Jan and Dan Duncan Neurological Research Institute, Texas Children's Hospital, Houston, TX 77030, USA. [7]Howard Hughes Medical Institute, Chevy Chase, MD 20815, USA.

*Present address: Department of Neuroscience, Mayo Clinic, FL 32224, USA.
†Present address: Laboratory of Cellular and Molecular Biology, National Cancer Institute, National Institutes of Health, Bethesda, MD 20892, USA.
‡To whom correspondence should be addressed. E-mail: hzoghbi@bcm.edu

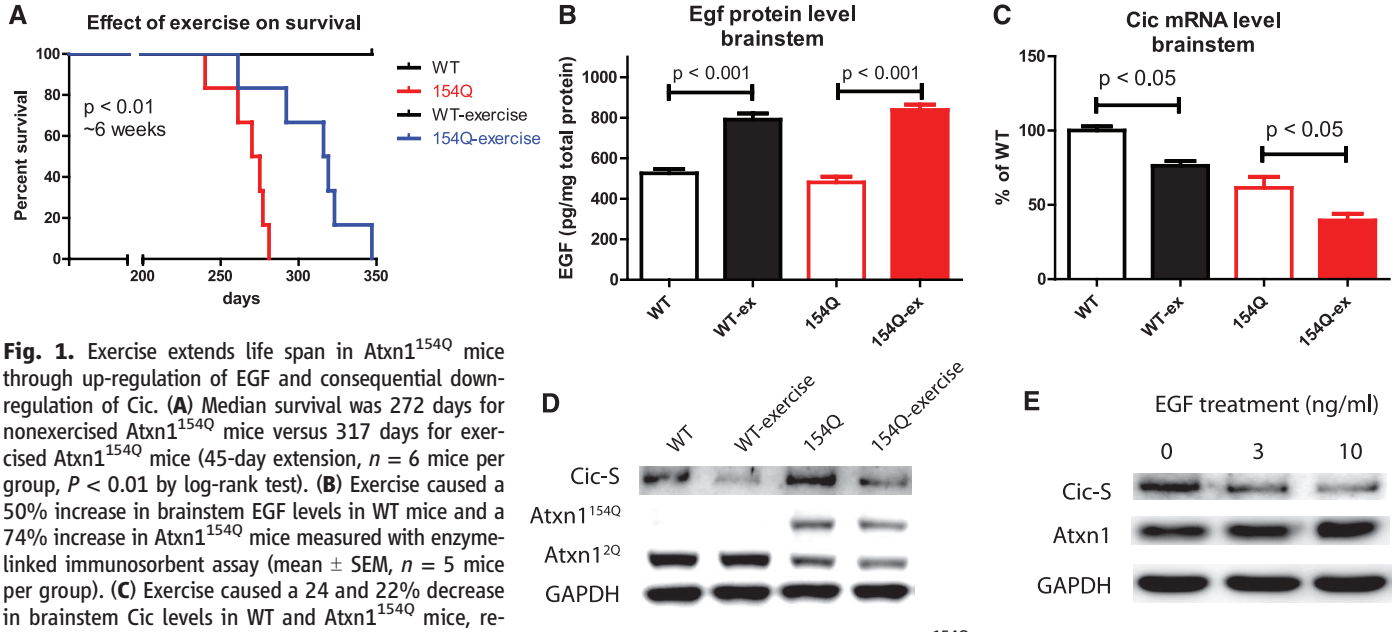

Fig. 1. Exercise extends life span in Atxn1^{154Q} mice through up-regulation of EGF and consequential down-regulation of Cic. (**A**) Median survival was 272 days for nonexercised Atxn1^{154Q} mice versus 317 days for exercised Atxn1^{154Q} mice (45-day extension, $n = 6$ mice per group, $P < 0.01$ by log-rank test). (**B**) Exercise caused a 50% increase in brainstem EGF levels in WT mice and a 74% increase in Atxn1^{154Q} mice measured with enzyme-linked immunosorbent assay (mean ± SEM, $n = 5$ mice per group). (**C**) Exercise caused a 24 and 22% decrease in brainstem Cic levels in WT and Atxn1^{154Q} mice, respectively, measured with quantitative reverse transcription polymerase chain reaction RT-PCR (mean ± SEM, $n = 5$ mice per group). (**D**) Western blotting for Cic demonstrates an exercise-induced decrease in Cic levels in the brainstem, whereas Atxn1 or Atxn1^{154Q} remain unaffected. (**E**) Primary brainstem neuronal cultures treated with recombinant EGF for 72 hours show a dose-dependent decrease in the level of Cic but not Atxn1.

Drosophila CENH3 Is Sufficient for Centromere Formation

María José Mendiburo, Jan Padeken, Stefanie Fülöp, Aloys Schepers and Patrick Heun

Science **334** (6056), 686-690.
DOI: 10.1126/science.1206880